Slope stability analysis and slope failure simulation by SPH

L'Analyse de Stabilité de Pente et la Simulation de la Rupture de Pente par SPH

H. H. Bui, K. Sako
Research Organization of Science and Engineering, Ritsumeikan University, Japan
R. Fukagawa
Department of Civil Engineering, Ritsumeikan University, Japan

ABSTRACT

In this paper, the SPH method is applied to evaluate stability of a slope and to simulate the gross discontinuities after failure. Herein, the Drucker-Prager model with non-associated plastic flow rule is employed to describe the elasto-plastic soil behaviour. The shear strength reduction method is applied to estimate the safety factor of a slope, while critical slip surface is automatically determined from contour plot of accumulated plastic strain. To take into account the pore-water pressure, a new SPH momentum equation is proposed. It is shown that by using this new expression of momentum equation, the free-surface boundary condition between water and submerged soil is automatically imposed without explicitly implementing a computational procedure to calculate an external force (pressure force). This paper suggests that the new SPH momentum equation developed herein is also applicable for further developments of SPH for saturated/unsaturated soils. As an application of the proposed method, slope stability analyses and slope failure simulations of a two-side earth embankment are performed and then comparing with traditional solutions. Very good agreements with limit equilibrium method and finite element method (FEM) have been obtained. This suggests that SPH is a promising method for the current application, especially for handling large deformation and failure of a slope subjected to heavy rainfall or earthquake loading.

RÉSUMÉ

Dans ce papier, la méthode SPH est appliquée pour évaluer la stabilité d'une pente et simuler des discontinuities à grande échelle après l'échec. Ici, le modèle de Drucker-Prager avec la règle non-associée d'écoulement plastique est employé pour décrire le comportement de sol elasto-de-plastique. La méthode de réduction de limite de cisaillement est appliquée pour estimer le facteur de sécurité d'une pente, alors que la surface critique de glissement est déterminée des courbes isovaleurs de deformation plastique accumulé. Pour tenir compte de la pression eau, une nouvelle équation dynamique SPH est proposée. Il est montré que grace à cette nouvelle expression, la condition de surface libre entre le sol et l'eau est automatiquement imposée sans calculer explicit de une force externe de pression (pression force). Nous suggère que cette nouvelle équation dynamique SPH sera utile pour pour divers applications futures de SPH aux sols saturés/non saturés. A titre d'exemple, la méthode est appliqué à l'analyse de stabilité des pente et aux simulations d'échec des pente de remblais de terre a deux côtés, et les resultats sont ensuite comparés avec les solutions traditionnelles. De très bons accords avec la méthode d'équilibre de limite et la simulation FEM ont été obtenus. Cela suggère que la SPH est une méthode prometteuse pour simuler des talus, surtout pour la grande déformation et la rupture des talus sous pluviometrie intense ou subissant des séismes.

Keywords : SPH (Smoothed particle hydrodynamics), large deformation, slope stability, slope failure, elasto-plasticity

1 INTRODUCTION

FEM has been considered as the standard numerical method for computational geomechanics. However, when dealing with large deformation and failure, FEM exhibits several disadvantages due to the grid distortion problem. Thus, the SPH method has been recently developed to resolve this limitation. SPH was originally invented for astrophysical applications (Lucy, 1977; Monaghan & Gingold 1977). Since its invention, it has been successfully applied to a vast range of problems such as dynamic response of material strength (Libersky et al. 1993), fluid flow (Monaghan 1994), etc. The recent SPH application to soil mechanics was performed by Maeda et al. (2004) in which a simple nonlinear elastic model was employed to simulate granular soil. Since then, many researchers have attempted to use SPH for large deformation and failure simulations of geomaterials. However, no implementations of SPH that solve plastic soil behaviour were available until our group implemented elasto-plastic soil constitutive models (Bui et al. 2007-2008), which has demonstrated successful performance of SPH for simulating such problems as slope failure, bearing capacity that are commonly found in geotechnical engineering. In this study, to enhance our proposed method for computational geomechanics, SPH is extended to evaluate stability of a slope and to simulate the gross discontinuities of soil after failure. Herein, the soil is modeled by the Drucker-Prager model with non-associated plastic flow rule. The shear strength reduction technique (Griffths et al., 1999) is applied to estimate the safety factor (*FOS*), while the critical slip surface is determined through contour plot of accumulated plastic strain. To take into account the pore-water pressure, new SPH governing equation is proposed to include accurate pore-pressure value. Herein, the gradient of pore-water pressure appeared in the momentum equation is approximated in the SPH formulation to ensure that the gradient of a constant pore-water pressure field is vanished. Finally, SPH is applied to model two-side earth embankment, which was analyzed by Griffths et al. (1999). Two study cases are considered throughout: homogeneous embankment with free surface, and embankment without free surface. Results are then compared with the limit equilibrium method and FEM (Griffths et al. 1999). Very good agreements in term of safety factors and critical slip surfaces have been obtained. However, the key issue of using the proposed method is that SPH can simulate whole

Proceedings of the 17th International Conference on Soil Mechanics and Geotechnical Engineering
M. Hamza et al. (Eds.)

doi:10.3233/978-1-60750-031-5-1578

failure process of the slope while such problem becomes troublesome with the traditional methods. This suggests that SPH is a promising method to simulate slopes especially for large deformation and failure of a slope subjected to heavy rainfall or earthquake loading.

2 SIMULATION APPROACHES

2.1 *Motion equation*

The motions of a continuum media can be described through the following equation,

$$\frac{dv^\alpha}{dt} = \frac{1}{\rho}\frac{\partial \sigma'^{\alpha\beta}}{\partial x^\beta} + f^\alpha \tag{1}$$

In the SPH framework, the above equation can be approximated through the use of a kernel interpolation, leading to

$$\frac{dv_i^\alpha}{dt} = \sum_{j=1}^{N} m_j \left(\frac{\sigma_i'^{\alpha\beta}}{\rho_i^2} + \frac{\sigma_j'^{\alpha\beta}}{\rho_j^2} \right) \frac{\partial W_{ij}}{\partial x^\beta} + f^\alpha \tag{2}$$

where i is the particle under consideration; N is the number of neighbouring particles, i.e. those in the support domain of particle i; m is the mass of particle; α and β denote Cartesian components x, y, z with the Einstein convention applied to repeated indices; ρ is the density; v is the velocity; σ' is the effective stress tensor; W_{ij} is the smoothing function. Herein the cubic spline function (Monaghan 1985) is adopted; and f^α is the external force.

As discussed by Bui et al. (2007), SPH encounters the so-called "tensile instability" problem when applied to cohesive soil. To remove this problem, they have proposed to use an artificial stress method, originally invented by Gray et al. (2001). Accordingly, equation (2) is modified to,

$$\frac{dv_i^\alpha}{dt} = \sum_{j=1}^{N} m_j \left(\frac{\sigma_i'^{\alpha\beta}}{\rho_i^2} + \frac{\sigma_j'^{\alpha\beta}}{\rho_j^2} + F_{ij}^n R_{ij}^{\alpha\beta} \right) \frac{\partial W_{ij}}{\partial x^\beta} + f^\alpha \tag{3}$$

where

$$F_{ij}^n R_{ij}^{\alpha\beta} = \left[\frac{W_{ij}}{W(d_o, h)} \right]^n (R_i^{\alpha\beta} + R_j^{\alpha\beta}) \tag{4}$$

where n is a parameter; d_0 is the initial distance between particles; h is the smoothing length, which specified the non-zero region of the smoothing function; and R_{ij} is obtained as follows. For each particle the effective stress tensor $\sigma'^{\alpha\beta}$ is diagonalised. Then an artificial stress term is evaluated for any of the diagonal components $\bar{\sigma}'^{\alpha\beta}$ which are positive,

$$\bar{R}_i^{\gamma\gamma} = -\varepsilon_0 \frac{\bar{\sigma}_i'^{\gamma\gamma}}{\rho_i^2} \tag{5}$$

where ε_0 is a small parameter ranging from 0 to 1. The artificial stress in the original coordinates system R_{ij} is then calculated by reverse coordinates transformation. Gray et al. (2001) derived optimal values from the dispersion equations, and suggested to use $\varepsilon_0 = 0.3$ and $n = 4$ when applied SPH to solid. However, Bui et al. (2008) showed that these selections can not remove the tensile instability problem found when simulating cohesive soil. Instead, they suggested to use $\varepsilon_0 = 0.5$ and $n = 2.55$, and proved that these values have no effect on the modeled soil behaviour. In this paper, the same values are applied.

Although the tensile instability problem can be removed by using the artificial stress term, results obtained from SPH may still suffer from stress fluctuation, which results from the non-uniform particle distribution in space when particles get too close to each other. This problem is actually found in most SPH applications to engineering practice. In order to damp out such unphysical stress fluctuation, an additional artificial viscosity term proposed by Monaghan (1983) is often added to the momentum equation. Accordingly, equation (3) is further modified to,

$$\frac{dv_i^\alpha}{dt} = \sum_{j=1}^{N} m_j \left(\frac{\sigma_i'^{\alpha\beta}}{\rho_i^2} + \frac{\sigma_j'^{\alpha\beta}}{\rho_j^2} + F_{ij}^n R_{ij}^{\alpha\beta} + \Pi_{ij}\delta^{\alpha\beta} \right) \frac{\partial W_{ij}}{\partial x^\beta} + f^\alpha \tag{6}$$

where

$$\Pi_{ij} = \begin{cases} \dfrac{-\alpha_\Pi c_{ij}\phi_{ij}}{\rho_{ij}} & (v_i - v_j)\cdot(x_i - x_j) < 0 \\ 0 & (v_i - v_j)\cdot(x_i - x_j) \geq 0 \end{cases} \tag{7}$$

where

$$\phi_{ij} = \frac{h(v_i - v_j)\cdot(x_i - x_j)}{|x_i - x_j|^2 + 0.01h^2} \tag{8}$$

In the above artificial viscous term $\prod_{ij}$, α_Π is a constant parameter which is set to be 0.1, and c is the sound speed, which should be chosen similar to Bui et al. (2008).

When considering the presence of water in soil media, it is necessary to take into account the pore-water pressure (p_w) into the momentum equation. Directly replacing the total stress tensor, which consists of effective stress and pore-water pressure, into equation (6) will result in numerical instability for soil particles near the submerged soil surface. To remove this problem, Bui et al. (2009) has derived a new SPH formulation of the momentum equation where the pore-water pressure is implemented in the following way,

$$\begin{aligned} \frac{dv_i^\alpha}{dt} = & \sum_{j=1}^{N} m_j \left(\frac{\sigma_i'^{\alpha\beta}}{\rho_i^2} + \frac{\sigma_j'^{\alpha\beta}}{\rho_j^2} + F_{ij}^n R_{ij}^{\alpha\beta} + \Pi_{ij}\delta^{\alpha\beta} \right) \frac{\partial W_{ij}}{\partial x^\beta} \\ & + \sum_{j=1}^{N} \frac{m_j}{\rho_i \rho_j} (p_{wj} - p_{wi}) \frac{\partial W_{ij}}{\partial x^\beta} + f^\alpha \end{aligned} \tag{9}$$

It is easy to see that this equation ensures that the gradient of a constant pore-water pressure field vanishes. Furthermore, the above expression of pore-water pressure automatically imposes the dynamic boundary condition at the free surface. For details of driving this equation, we refer the readers to our coming publication (Bui et al. 2009). Finally, the above motion equation can be solved directly using the standard Leapfrog algorithm if the effective stress tensor is known. Thus, it is necessary to derive constitutive equations for the effective stress tensor that are applicable in the SPH framework.

2.2 *Soil constitutive modeling*

According to the classical plasticity theory, the total strain rate tensor of an elasto-plastic material is decomposed into two parts: an elastic strain rate tensor and a plastic strain rate tensor,

$$\dot{\varepsilon}^{\alpha\beta} = \dot{\varepsilon}_e^{\alpha\beta} + \dot{\varepsilon}_p^{\alpha\beta} \tag{10}$$

The elastic strain rate tensor is given by a generalized Hooke type of law, i.e.,

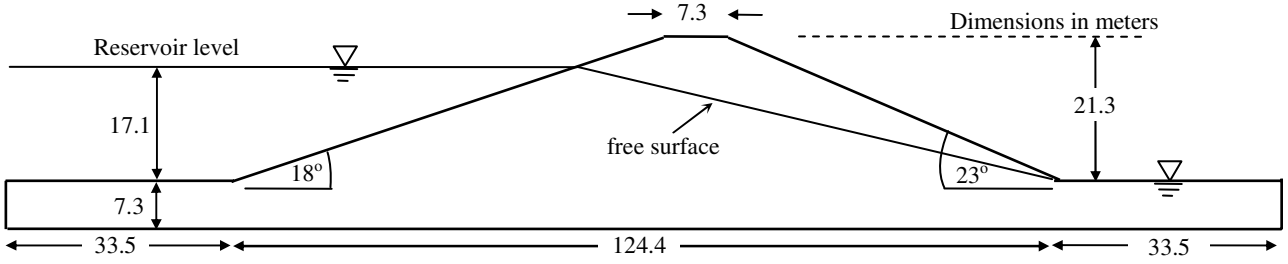

Figure 1: Two-side earth embankment model (Griffths et al. 1999)

$$\dot{\varepsilon}_e^{\alpha\beta} = \frac{\dot{s}'^{\alpha\beta}}{2G} + \frac{1-2\upsilon}{E}\dot{\sigma}'^{m}\delta^{\alpha\beta} \tag{11}$$

where $s'^{\alpha\beta}$ is the deviatoric effective shear stress tensor; υ is Poisson's ratio; E is the elastic Young's modulus; G is the shear modulus and σ'^{m} is the effective mean stress.

The plastic strain rate tensor is calculated by the plastic flow rule, which is given by

$$\dot{\varepsilon}_p^{\alpha\beta} = \dot{\lambda}\frac{\partial g}{\partial \sigma'^{\alpha\beta}} \tag{12}$$

where $\dot{\lambda}$ is the rate of change of plastic multiplier, and g is the plastic potential function.

In the current study, the Drucker-Prager model with non-associated flow rule is applied to model the soil. In addition, this study assumes that the yield surface is fixed in stress space. Accordingly, the plastic deformation will occur only if the following yield criterion is satisfied,

$$f(I_1, J_2) = \sqrt{J_2} + \alpha_\phi I_1 - k_c = 0 \tag{13}$$

where I_1 and J_2 are, respectively, the first and second invariants of stress tensor; α_ϕ and k_c are the Drucker-Prager constants, which are calculated by,

$$\alpha_\phi = \frac{\tan\phi}{\sqrt{9+12\tan^2\phi}} \quad \text{and} \quad k_c = \frac{3c}{\sqrt{9+12\tan^2\phi}} \tag{14}$$

where c is the cohesion and ϕ is the internal friction angle. For the non-associated plastic flow rule, the plastic potential function is given by,

$$g = 3I_1\sin\psi + \sqrt{J_2} \tag{15}$$

Substituting equations (11), (12) into (10), and adopting the Jaumman stress rate for large deformation treatment, the stress-strain relation for the current soil model at particle i becomes,

$$\begin{aligned}\frac{d\sigma_i'^{\alpha\beta}}{dt} &= \sigma_i'^{\alpha\gamma}\dot{\omega}_i^{\beta\gamma} + \sigma_i'^{\gamma\beta}\dot{\omega}_i^{\alpha\gamma} + 2G_i\dot{e}_i^{\alpha\beta} + K_i\dot{\varepsilon}_i^{\gamma\gamma}\delta_i^{\alpha\beta} \\ &\quad - \dot{\lambda}_i\left[9K_i\sin\psi_i\,\delta^{\alpha\beta} + (G/\sqrt{J_2})_i s_i'^{\alpha\beta}\right]\end{aligned} \tag{16}$$

where $\dot{e}^{\alpha\beta}$ is the deviatoric shear strain rate tensor; ψ is the dilatancy angle; $\dot{\lambda}$ is the rate of change of plastic multiplier, which in SPH is specified by,

$$\dot{\lambda}_i = \frac{3\alpha_\phi K\dot{\varepsilon}_i^{\gamma\gamma} + (G/\sqrt{J_2})_i s_i'^{\alpha\beta}\dot{\varepsilon}_i^{\alpha\beta}}{27\alpha_\phi K_i\sin\psi_i + G_i} \tag{17}$$

and $\dot{\varepsilon}_i^{\alpha\beta}$, $\dot{\omega}_i^{\alpha\beta}$ are respectively the strain rate and spin rate tensors defined by,

$$\dot{\varepsilon}_i^{\alpha\beta} = \frac{1}{2}\left(\frac{\partial v^\alpha}{\partial x^\beta} + \frac{\partial v^\beta}{\partial x^\alpha}\right)_i \quad \text{and} \quad \dot{\omega}_i^{\alpha\beta} = \frac{1}{2}\left(\frac{\partial v^\alpha}{\partial x^\beta} - \frac{\partial v^\beta}{\partial x^\alpha}\right)_i \tag{18}$$

The above soil constitutive model requires six soil parameters, which are the cohesion coefficient (c), friction angle (ϕ), dilation angle (ψ), and Young's modulus (E), Poisson's ratio (υ), and soil density (ρ).

2.3 *Shear strength reduction method*

To calculate the safety factor of a slope defined by the shear strength reduction technique (Griffths et al., 1999), a series of stability analyses are performed with reduced shear strength parameters c_t and ϕ_t defined as follows,

$$c_t = \frac{c}{FOS^t} \quad \text{and} \quad \phi_t = \boldsymbol{arctan}\left(\frac{\tan\phi}{FOS^t}\right) \tag{19}$$

where c and ϕ are real shear strength parameters, and FOS^t is the trial safety factor. Normally, initial FOS^t is set to be sufficiently small so that the system is stable. Then, the value of FOS^t is increased gradually until the slope fails. The final value of FOS^t that makes the slope fail is defined as the safety factor of the slope, which is identical to the one in limit equilibrium method.

3 NUMERICAL APPLICATIONS

To validate the proposed method for slope stability analysis and slope failure simulation, the two-side earth embankment model analyzed by Griffths et al. (1999) is employed herein, Figure 1. The embankment is assumed to be made of homogeneous soil with $E = 10^5$kN/m^2, $\upsilon = 0.3$, $\phi = 37^o$, $c = 13.8$kN/m^2, and $\gamma = 18.2$kN/m^3 (below and above the free surface). The boundary conditions consist of vertical rollers on the faces at the left and right ends and full fixity at the base of the foundation layer. According to Griffths et al. (1999), FEM analyses gave FOS = 2.4 for the slope without considering free surface and FOS = 1.9 for the slope with free surface. These results are in close agreement with limit equilibrium analyses, which gave FOS = 2.42 for the slope without free surface and FOS = 1.9 for the slope with free surface.

The SPH results of slope stability analysis by shear strength reduction technique are shown in Figure 2. It can be seen that computation is unconvergent when FOS^t = 2.4 for the slope without free surface and FOS^t = 1.9 for the slope with free surface. These values of FOS^t are considered as the safety factors of the current slopes, which are in very close agreement with FEM and limit equilibrium analyses obtained by Griffths et al. (1999). It is noted that for the case with free surface, the pore-water pressure was calculated as the product between unit weight (γ_w) of water and the vertical distance of particle beneath the free surface. The more accurate pore-water pressure distribution can be obtained by solving the seepage flow

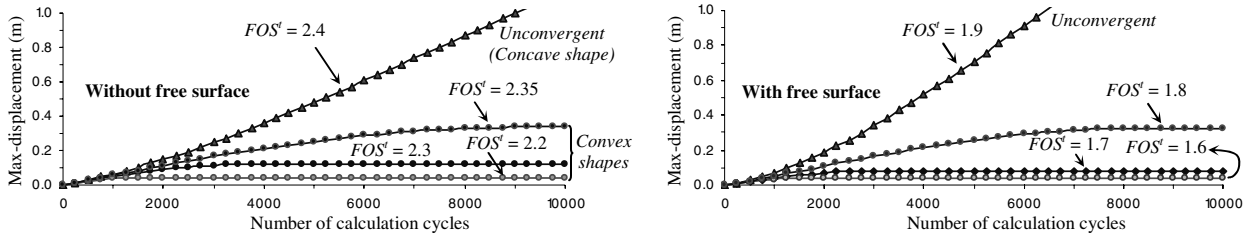

Figure 2: Convergent/unconvergent analyses of slope stability via the shear strength reduction technique by SPH.

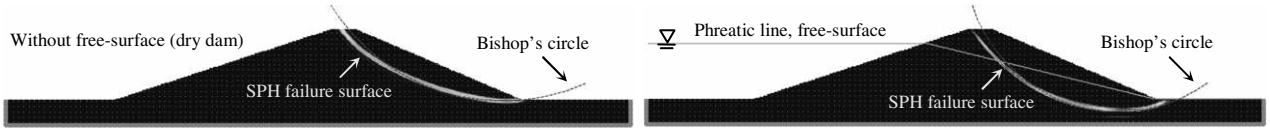

Figure 3: Critical slip surfaces obtained from SPH (color band) and limit equilibrium method (red dash-line).

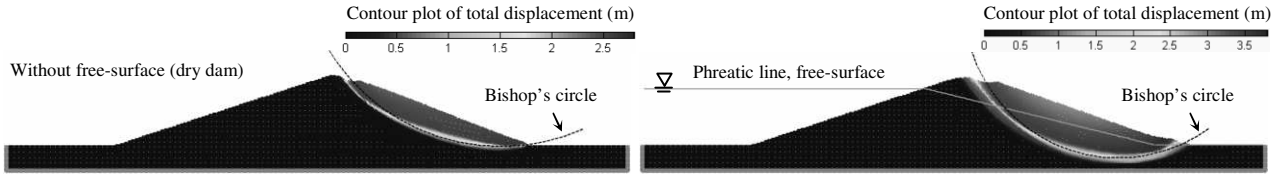

Figure 4: Final configurations of the slopes corresponding to the unconvergent SPH solutions.

equation using either FEM or SPH. Such works are postponed to a future publication.

Regarding the critical slip surface, Figure 3 shows the contour plot of accumulated plastic strain corresponding to unconvegent SPH solutions as compared to the circle slip surface obtained from the limit equilibrium method (Griffths et al., 1999). As expected, the failure occurs on the steeper, downstream side of the embankment in both cases. Again, close agreements are obtained between SPH and the limit equilibrium method. The slight difference between two methods can be explained due to the assumption of circle slip surface in the limit equilibrium method though almost similar result was obtained for the case without free surface. In addition, the toe failure mechanism is also observed in SPH with a deeper mechanism extending into the foundation layer for the case with a free surface.

Figure 4 shows the final configuration of the slopes after collapse, via contour plot of total displacements. The gross discontinuous failure along the slip surface, which is unable to model by FEM, can be now described very well by SPH. Numerical simulation can be performed as long as desired without encountering any problems. Furthermore, comparison between two cases shows that the failure zone is enlarged for the case with a free surface. This result is also similar to what obtained by Griffths et al. (1999).

4 CONCLUSIONS

This work presented a new approach for slope stability analysis and slope failure simulation using the SPH method. Herein, the Drucker-Prager model with non-associated plastic flow rule is applied to describe the elasto-plastic soil behavior. The shear strength reduction method is employed to estimate the safety factor of the slope, while the critical slip surface is decided through the contour plot of accumulated plastic strain. Furthermore, a new SPH momentum equation was also proposed to include accurate pore-water pressure into the momentum equation. Results obtained from this study show that SPH could give good agreements with FEM and the limit equilibrium method in term of the safety factor and critical mechanism of failure. However, the advantage of using SPH, which is over FEM and the limit equilibrium method, is that it can simulate the whole failure process of the slope. This suggests that SPH is a promising method for the current applications, especially for large deformation and failure of a slope subjected to heavy rainfall or earthquake loading. The new SPH equation proposed in this paper can be considered as the basic equation for future implements of such purposes.

REFERENCES

Bui, H.H. 2007. Lagrangian mesh-free particle method (SPH) for large deformation and post-failure of geomaterial using elasto-plastic soil constitutive models, *PhD. Thesis, Department of Civil Engineering, Ritsumeikan University, Japan*.

Bui, H.H. Sako, K. & Fukagawa, R. 2007. Numerical simulation of soil-water interaction using smoothed particle hydrodynamics, *Journal of Terramechanics* 44(5):165-175.

Bui, H.H. Fukagawa, R. Sako, K. & Ohno, S. 2008. Lagrangian mesh-free particle method (SPH) for large deformation and post-failure of geomaterials using elastic-plastic soil constitutive model, *International Journal for Numerical and Analytical Methods in Geomechanics* 32(12): 1537-1570.

Bui, H.H. Fukagawa, R. Sako, K. & Wells, J.C. 2009. Slope stability analysis and discontinuous slope failure simulation by elasto-plastic smoothed particle hydrodynamics (SPH), *Geotechnique* (submitting).

Gingold, R.A. & Monaghan, J.J. 1977. Smoothed particle hydrodynamics: Theory and application to non spherical stars. *Mon. Not. Roy. Astron. Soc.* 181: 375-389.

Gray, J.P. Monaghan, J.J. & Swift, R.P. 2001. SPH elastic dynamics. *Computer Methods in Applied Mechanics and Engineering* 190: 6641-6662.

Griffths, D.V. & Lane, P.A. 1999. Slope stability analysis by finite elements. *Geotechnique* 49(3):387-403.

Maeda, K. & Sakai, M. 2004. Development of seepage failure analysis procedure of granular ground with SPH. *Journal of Applied Mechanics JSCE* 7:775-786. (in Japanese)

Monaghan, J.J. Lattanzio, J.C. 1985. A refined particle method for astrophysical problems. *Astronomic and Astrophysics* 149:135-143.

Libersky, L.D. Petschek, A.G. Carney, T.C. Hipp, J.R. & Allahdadi, F.A. 1993. High Strain Lagrangian Hydrodynamics: A Three Dimensional SPH Code for Dynamic Material Response. *Journal of Computational Physics* 109:67-75.

Lucy L.1977. A Numerical approach to testing the fission hypothesis. *Astronomical Journal* 82:1013-1024.